# Supplementary Material for "Distortions to the penetration depth and coherence length of superconductor/normal-metal superlattices" by P. Quarterman *et al.*

X-ray reflectivity is collected on the samples uing a Cu-K$\alpha$ source (supplementary Fig. S1(a)), and the resulting fits to the data yield scattering length density profiles, shown in supplementary Fig. S1(b), in strong agreement with the polarized neutron reflectometry results. From the PNR and XRR we find that thicknesses for Nb/Al and Nb/Au superlattice samples are 25.2 nm / 2.5 nm and 23.6 nm / 1.7 nm, respectively. The single layer of Nb is found to be 188 nm. Off-specular scattering is collected to use for background subtraction by offsetting $\theta$ and scanning $\theta-2\theta$ in order to sample the $Q_z$ dependence of the in-plane disorder (Fig. S1(c)). For the off-specular background scattering in the Nb sample, we observe no $Q$-dependent oscillations, as expected. However, in the superlattices the background scans show strong periodic oscillations. These off-specular oscillations have been shown to be indicative of conformal roughness [1,2].

Rocking curves are shown for the Nb, Nb/Al, and Nb/Au samples in Fig. S2. The Nb rocking curve at $2\theta = 1.2^\circ$ shows pronounced peaks (Yoneda wings) near $\theta \approx \theta_C$ and $2\theta$ - $\theta_C$, where $\theta_C$ is the critical angle. These Yoneda peaks are suggestive of significant surface roughness [3]. In contrast, the only pronounced peaks observed in the Nb/Al and Nb/Au rocking curves are the specular reflections, which are on top of broad diffuse scattering for the latter sample. In the Nb/Au rocking curve at $2\theta = 1.3^\circ$, there are peak-like artifacts symmetric about the specular reflection. In the rocking curve measured at $2\theta = 2.2^\circ$, however, these features do not shift outward in a manner consistent with Yoneda scattering. In qualitative comparison to those of the Nb film, the surfaces of the Nb/N superlattices appear to be relatively smooth on a local scale.

The spin asymmetry for the Nb/Al superlattice taken at 20 K is shown in supplemental Fig. S3, and as expected we see no observable magnetic contribution to the PNR. Similar observations are seen for the Nb and Nb/Au samples taken when measured above the superconducting critical temperature of the samples. We utilize a Markov chain Monte Carlo method, known as DREAM [4], which allows us to precisely determine uncertainties for numerous correlated parameters. We note that the uncertainties reported for our fit parameters do not account for deficiencies in the model or all of the systematic error that

might be associated with the experiment. However, based on the theoretical plausibility of our model, and the overall goodness of fit we conclude that such unaccounted contributions to the total uncertainty are quite small, and that our model is a reasonable representation of reality. To demonstrate the robustness of our model-fitting of the penetration depth, we have carried out additional fitting where $\lambda_L$ is fixed to a series of values, and the scattering length densities, layer thicknesses, and interfacial roughnesses are fit (as used for main text). These alternative fits are shown in supplementary Fig. S4. In the Nb/Al sample, we find that the magnetic contribution to the model-fitting is dominated by the features near $Q = 0.14$ and 0.25 nm$^{-1}$, and when $\lambda_L$ is too small the theoretical model over estimates the spin asymmetry near $Q = 0.25$ nm$^{-1}$, whereas if $\lambda_L$ is too large, the model does not capture the dip near $Q = 0.14$ nm$^{-1}$. Thus, we can qualitatively understand the fit as balancing these two features for a minimization in $\chi^2$. We observe a similar balancing of the first low $Q$ dip (0.14 nm$^{-1}$) with oscillations at higher $Q$, in the spin asymmetry, for the Nb/Au sample.

We determine the upper critical fields ($H_{c2\parallel}$ and $H_{c2\perp}$) by measuring resistance as a function of field ($R$ vs. $H$); typical $R$ vs. $H$ curves for the field applied in-plane and out-of-plane are shown in supplemental Fig. 5. $H_{c2}$ is determined by taking the peak of the first derivative of the resistance with respect to field, and averaging the result obtained at the positive and negative field regime.

In the main text, we define several coherence lengths in our system. One such length that we do not consider in the main text is the normal state effective coherence length inside the $N$ layers ($\xi_N$). To provide an estimate for $\xi_N$ in the diffusive (dirty) limit for Al and Au, we can follow Buzdin [5],

$$\xi_N = \sqrt{\frac{\hbar D}{2\pi k_B T}}, \tag{1}$$

where $D$ is the diffusion coefficient, $D = \frac{1}{3} v_{\mathrm{F}} l$, and $v_{\mathrm{F}}$ and $l$ are the Fermi velocity and mean free path respectively. Values for $v_{\mathrm{F}}$ and $l$ are taken from Gall [6], with the limitation that $l$ is calculated by Gall at room temperature. We estimate the normal metal effective coherence length for Al and Au at 3 K, associated with the proximity effect, in the diffusive limit to be $\xi_N = 65$ nm and $\xi_N = 85$ nm.

[1] H. Zabel, Appl. Phys. A. **58**, 159 (1994).

[2] J. M. Freitag and B. M. Clemens, J. Appl. Phys. **89**, 1101 (2001).

[3] D. E. Savage, J. Kleiner, N. Schimke, Y. Phang, T. Jankowski, J. Jacobs, R. Kariotis, and M. G. Lagally, J. Appl. Phys **69**, 1411 (1991).

[4] J. A. Vrugt, C. J. F. ter Braak, C. G. H. Diks, B. A. Robinson, J. M. Hyman and D. Higdon, Int. J. Nonlin. Sci. Num. **10** 273 (2009)

[5] A. I. Buzdin, Rev. Mod. Phys. **77**, 935 (2005).

[6] D. Gall, J. Appl. Phys **119**, 085101 (2016).

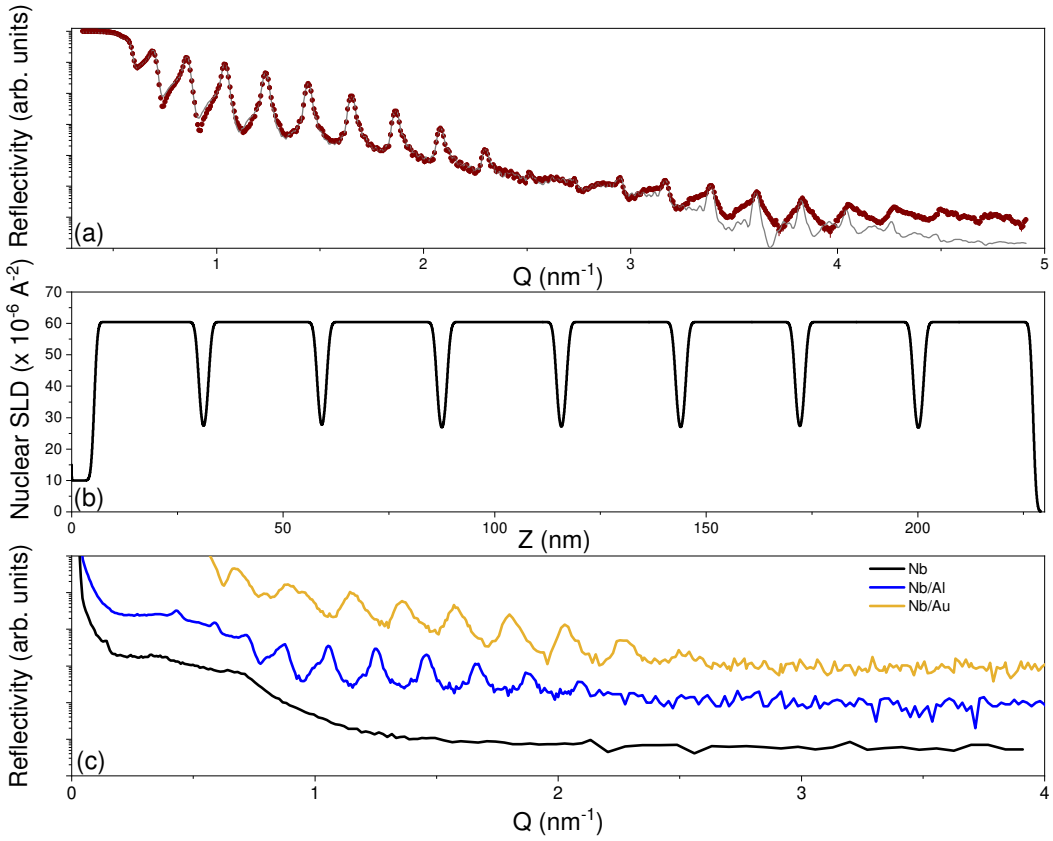


FIG. S1. (a) XRR data and model for Nb/Al, with a corresponding SLD profile shown in (b). (c) Off-specular x-ray reflectivity for the Nb, Nb/Al and Nb/Au samples. The superlattices show pronounced oscillations in the off-specular signal, which are indicative of conformal roughness.

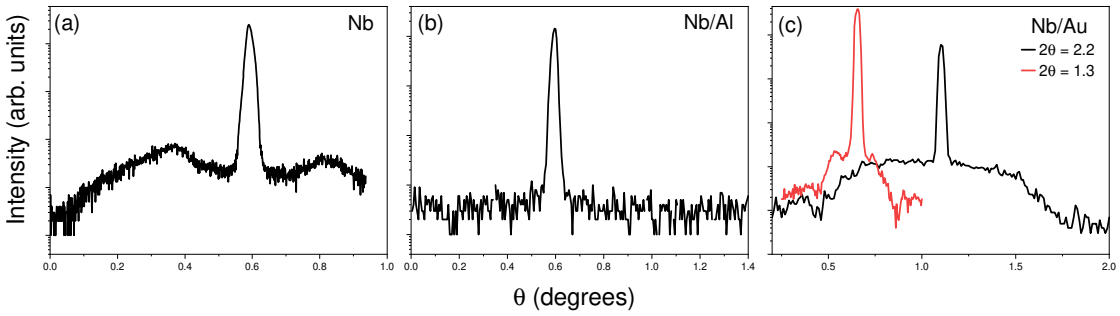


FIG. S2. X-ray rocking curves of (a) Nb, (b) Nb/Al, and (c) Nb/Au samples. The Nb and Nb/Al rocking curves were obtained at $2\theta = 1.2°$. Rocking curves for Nb/Au were measured at $2\theta = 1.3°$ for direct comparison to (a) and (b) and at $2\theta = 2.2°$ at the maximum of a specular superlattice peak. A comparison of these two curves suggests that the apparent features in the diffuse scattering are not consistent with Yoneda scattering.

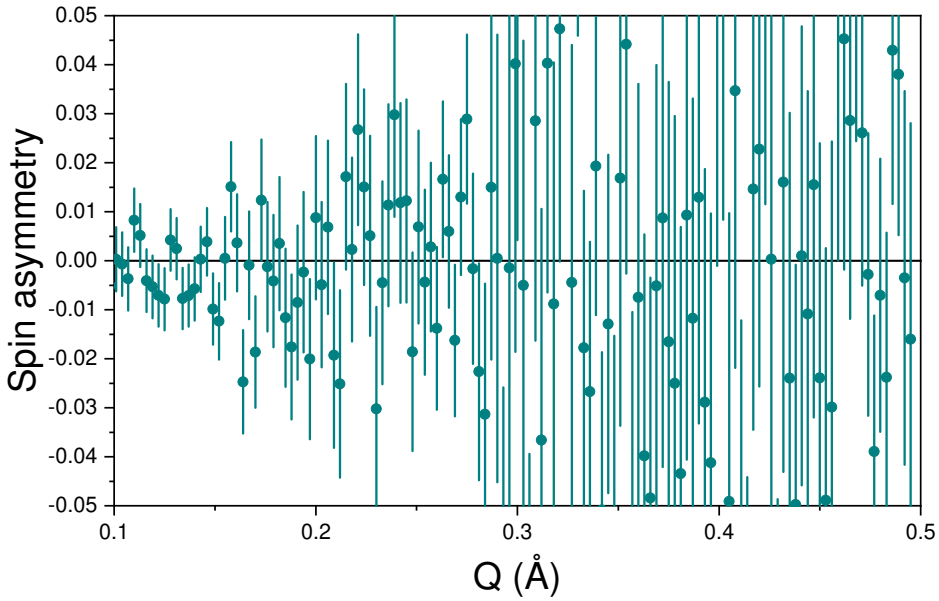


FIG. S3. Spin asymmetry for Nb/Al superlattice collected at 20 K, which is above the superconducting critical temperature of the sample. Error bars are representative of $1\sigma$

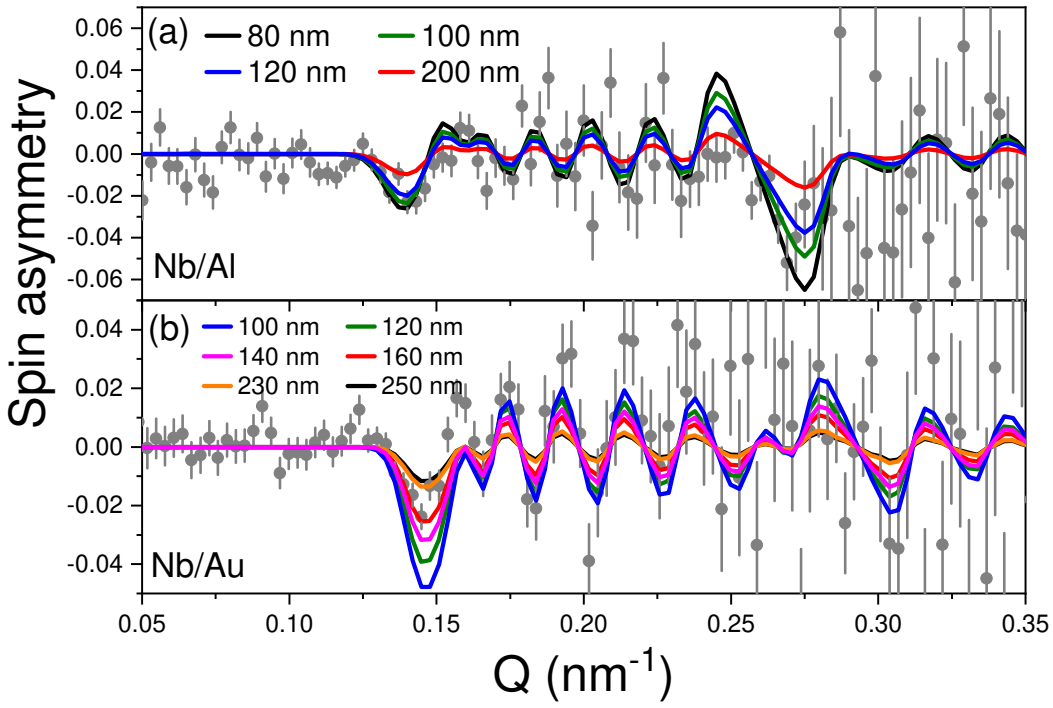


FIG. S4. Spin asymmetry for (a) Nb/Al and (b) Nb/Au superlattice collected at 3 K, where modeling was done by fixing $\lambda_L$ (see legend) outside of the fit error range to highlight where model-fitting fails when $\lambda_L$ is either too large or too small. Error bars are representative of $1\sigma$

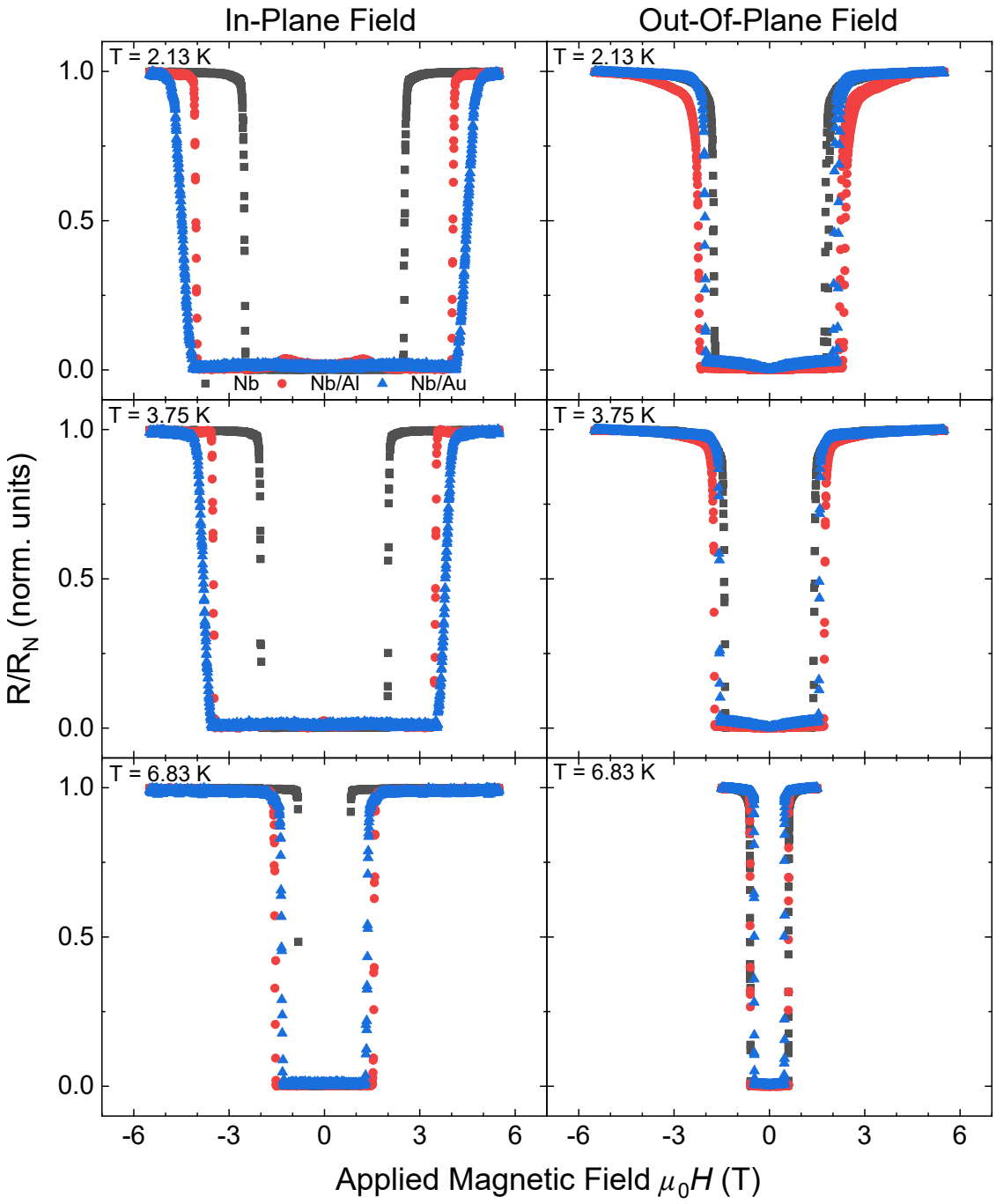


FIG. S5. Resistance vs magnetic field for the Nb (black, squares), Nb/Al (red, circles), and Nb/Au (blue, triangles) samples to determine $H_{c2\parallel}$ and $H_{c2\perp}$.